

## ORIGINAL ARTICLE

# A potent neutralizing nanobody against SARS-CoV-2 with inhaled delivery potential

Junwei Gai<sup>1</sup> | Linlin Ma<sup>2</sup> | Guanghui Li<sup>1</sup> | Min Zhu<sup>1</sup> | Peng Qiao<sup>1</sup> |  
 Xiaofei Li<sup>1</sup> | Haiwei Zhang<sup>3</sup> | Yanmin Zhang<sup>4</sup> | Yadong Chen<sup>4</sup> | Weiwei Ji<sup>1</sup> |  
 Hao Zhang<sup>1</sup> | Huanhuan Cao<sup>1</sup> | Xionghui Li<sup>1</sup> | Rui Gong<sup>3</sup> | Yakun Wan<sup>1</sup>

<sup>1</sup> Shanghai Novamab Biopharmaceuticals Co., Ltd, Shanghai, China

<sup>2</sup> Shanghai Key Laboratory of Molecular Imaging, Shanghai University of Medicine and Health Sciences, Shanghai, China

<sup>3</sup> CAS Key Laboratory of Special Pathogens and Biosafety, Wuhan Institute of Virology, Center for Biosafety Mega-Science, Chinese Academy of Sciences, Wuhan, China

<sup>4</sup> Laboratory of Molecular Design and Drug Discovery, School of Science, China Pharmaceutical University, Nanjing, China

## Correspondence

Yakun Wan, Shanghai Novamab Biopharmaceuticals Co., Ltd., Room 201, No. 10, Lane 500, FuRong Hua Road, Shanghai 201318, China.

Email: [ykwan@novamab.com](mailto:ykwan@novamab.com)

Rui Gong, CAS Key Laboratory of Special Pathogens and Biosafety, Wuhan Institute of Virology, Center for Biosafety Mega-Science, Chinese Academy of Sciences, No. 44, Xiaohongshan, Wuchang District, Wuhan 430071, China.

Email: [gongr@wh.iov.cn](mailto:gongr@wh.iov.cn)

Junwei Gai, Linlin Ma, Guanghui Li, Min Zhu, Peng Qiao, Xiaofei Li, and Haiwei Zhang contribute equally to this work.

## Funding information

National Natural Science Foundation of China, Grant/Award Number: 81902052; Shanghai Sailing Program, Grant/Award Number: 20YF1434300; Natural Science Foundation of Hubei Province of China, Grant/Award Number: 2019CFA076

## Abstract

The coronavirus disease 2019 (COVID-19) pandemic has become a serious burden on global public health. Although therapeutic drugs against COVID-19 have been used in many countries, their efficacy is still limited. We here reported nanobody (Nb) phage display libraries derived from four camels immunized with the SARS-CoV-2 spike receptor-binding domain (RBD), from which 381 Nbs were identified to recognize SARS-CoV-2-RBD. Furthermore, seven Nbs were shown to block interaction of human angiotensin-converting enzyme 2 (ACE2) with SARS-CoV-2-RBD variants and two Nbs blocked the interaction of human ACE2 with bat-SL-CoV-WIV1-RBD and SARS-CoV-1-RBD. Among these candidates, Nb11-59 exhibited the highest activity against authentic SARS-CoV-2 with 50% neutralizing dose (ND<sub>50</sub>) of 0.55 µg/ml. Nb11-59 can be produced on large scale in *Pichia pastoris*, with 20 g/L titer and 99.36% purity. It also showed good stability profile, and nebulization did not impact its stability. Overall, Nb11-59 might be a promising prophylactic and therapeutic molecule against COVID-19, especially through inhalation delivery.

## KEYWORDS

large-scale production, nanobody, nebulization, neutralizing activity, SARS-CoV-2

## 1 | INTRODUCTION

The world-wide spread of coronavirus disease 2019 (COVID-19) caused by SARS-CoV-2 is the third major coronavirus outbreak in the past 20 years. SARS-CoV-

2 is closely related to SARS-CoV, several SARS-like bat CoVs, and pangolin coronaviruses.<sup>1,2</sup> However, SARS-CoV-2 demonstrates a higher human-to-human transmissibility than SARS-CoV. Patients with confirmed SARS-CoV-2 infection had mild to severe respiratory illness

This is an open access article under the terms of the [Creative Commons Attribution](https://creativecommons.org/licenses/by/4.0/) License, which permits use, distribution and reproduction in any medium, provided the original work is properly cited.

© 2021 The Authors. *MedComm* published by Sichuan International Medical Exchange & Promotion Association (SCIMEA) and John Wiley & Sons Australia, Ltd.

with symptoms of fever, cough, headache, dyspnea, and pneumonia.<sup>3</sup> To date, treating this infection is still a big challenge.

Similar to other coronaviruses, the spike (S) glycoprotein homotrimer on the SARS-CoV-2 plays a pivotal role in receptor binding and viral entry.<sup>4</sup> The spike glycoprotein contains two functional subunits, termed S1 and S2. The S1 subunit is responsible for the binding of host cell receptor via the interaction between its C-terminal receptor-binding domain (RBD) and human angiotensin-converting enzyme 2 (ACE2). S2 subunit plays an important role in fusion of the viral and cellular membranes. The receptor binding, proteolytic processing, and structural rearrangement of S protein are regarded as the key events during the merging of the viral envelope with host membranes.<sup>5</sup> Crystal structure of SARS-CoV-2-RBD in complex with human ACE2 has been solved, which provides the basis for development of SARS-CoV-2-targeting vaccines and therapeutics.<sup>6</sup>

Heavy-chain-only antibodies (HCAbs) isolated from camels provide an alternative paradigm in development of therapeutic antibodies. HCAbs consist of only two heavy chains without light chains, thereby only containing a single variable domain (VHH) referred to as a single-domain antibody or nanobody (Nb) in the absence of the effector domain.<sup>7</sup> In addition to having affinities and specificities for antigens similar to those of traditional antibodies, Nbs show smaller size and higher stability than most antibodies.<sup>8</sup> Given these biophysical advantages, Nbs can be easily nebulized and delivered directly to lungs via an inhaler, which makes Nbs a particularly promising format for developing neutralizing antibodies targeting respiratory pathogens including SARS-CoV-2.<sup>9,10</sup>

Here, we report Nb phage display libraries derived from four camels immunized with the SARS-CoV-2 spike RBD. We identified a monovalent Nb, Nb11-59, with potent neutralizing activities against authentic SARS-CoV-2 in vitro, and Nb11-59 might be easily delivered by nebulization considering its small size and high stability.

## 2 | MATERIALS AND METHODS

### 2.1 | Cells and viruses

The HEK 293 and Vero E6 cells were obtained from the American Type Culture Collection (ATCC) and China Center for Type Culture Collection (CCTCC), respectively. The Vero E6 cells were grown in Dulbecco's Modified Eagle Medium (DMEM) (Gibco, GrandIsland, NY, USA) supplementing with 1% penicillin-streptomycin (10,000 U/ml) (Gibco) and 10% FBS (Gibco). The HEK 293 were grown in DMEM supplemented with 1% penicillin-streptomycin

and 10% FBS for Nbs functional analysis, and in CD05 (OPEM, SH, CN) for proteins production. The SARS-CoV-2 strain IVCAS 6.7512 was offered by the National Virus Resource, Wuhan Institute of Virology, Chinese Academy of Science.<sup>11</sup> All processes in this study involving authentic SARS-CoV-2 were performed in a biosafety level 3 (BSL-3) facility. The illustrations of authentic SARS-CoV-2 in Graphical Abstract was derived from the source page: Desiree Ho for the Innovative Genomics Institute.

### 2.2 | Phage display library construction and Nbs biopanning

The coding sequence of SARS-CoV-2 spike RBD was achieved from the UniProt website (<https://www.uniprot.org/>). The RBDs (residues 319–541) of SARS-CoV-2 spike with 10× his tag at N terminal were expressed in HEK 293 and purified with Ni-NTA affinity columns (Qiagen, Hilden, Germany). The RBDs of SARS-CoV-2 spikes were used as antigens to conduct camel immunization, and then the immunized phage display library was generated according to our established methods.<sup>12</sup> Briefly, four camels were injected with RBD antigens once every 5 days for a total of seven times. The peripheral blood from these immunized camels was collected for lymphocytes cells extraction and phage libraries were constructed. All procedures were performed according to the Health guide for the care and use of laboratory animals.

Phage display technology was used to perform Nbs biopanning. RBD with his tag was diluted in 100 mM NaHCO<sub>3</sub> and coated in microplate overnight. After blocking with BSA, the phages from the immunized library were added into wells for incubation. The specific phages were eluted after strict and harsh wash procedure to remove the unspecific binders. The specific phages would be enriched and prepared for the next round of biopanning.

### 2.3 | Periplasmic extract ELISA (PE-ELISA)

In order to identify positive clones, 400 clones from each of the four libraries were randomly picked and expressed in microplate for PE-ELISA verification. Each clone was cultured in Terrific Broth medium (Invitrogen) for 3 h and induced by 1 mM IPTG (Sigma-Aldrich, USA) overnight. After an osmotic shock, the supernatants were transferred into wells of the microtiter plate coated with SARS-CoV-2-RBD-His in advance. The mouse anti-HA antibody (Covance, Princeton, NJ, USA) and goat anti-mouse IgG-alkaline phosphatase (Sigma-Aldrich) were added to the wells for incubation successively. Then, 405 nm

absorbance was read by the microplate reader (Bio-Rad, Hercules, CA, USA) after the substrate of alkaline phosphatase was added. The positive clones were identified when the ratios were higher than 3.

## 2.4 | Nbs expression and purification

After sequencing the selected clones, the SARS-CoV-2-RBD-specific clones were amplified, and then the plasmids of these candidates were extracted and transformed into *Escherichia coli* strain WK6. Ni-NTA affinity columns (Qia-gen, Hilden, Germany) were used in purification of Nbs. Purified Nbs were confirmed through SDS-PAGE. For phylogenetic tree, the multiple alignment and the construction of the tree was made by Clustal Omega, and pair-wise distance was calculated by the strategy of Neighbor-joining.<sup>13</sup>

## 2.5 | Affinity determination

The kinetics of Nbs binding to SARS-CoV-2-RBD antigen were performed by biofilm interferometry (BLI) with a ForteBio's Octet RED96 instrument (ForteBio, Menlo Park, CA, USA). Briefly, the diluted Nbs (10  $\mu\text{g}/\text{ml}$ ) were coupled to protein A biosensors and then incubated with a series diluted SARS-CoV-2-RBD, followed by dissociation in PBST. The binding curves were fit in 1:1 binding model by Octet Data Analysis software 9.0. The association and dissociation rates were monitored and the equilibrium dissociation constant ( $K_d$ ) was determined.

## 2.6 | Activity assay of Nbs binding to SARS-CoV-2-RBD

To determine the activity of anti-SARS-CoV-2-RBD Nbs binding to the antigen of RBD, series diluted anti-SARS-CoV-2-RBD Nbs were incubated with 1  $\mu\text{g}/\text{ml}$  SARS-CoV-2-RBD-His coated on the 96 microtiter plate wells for 1 h. Next, the plates were incubated with the mouse anti-HA antibody followed by goat anti-mouse IgG-alkaline phosphatase (Sigma-Aldrich). The absorbance at 405 nm was read by the microplate reader (Bio-Rad, Hercules, CA, USA), and the 50% effective concentration ( $\text{EC}_{50}$ ) was determined.

## 2.7 | Activity assay of Nbs blocking SARS-CoV-2-RBD/ACE2

To determine the activity of anti-SARS-CoV-2-RBD Nbs blocking SARS-CoV-2-RBD/ACE2 interaction,

ACE2/HEK 293 stable cell line was constructed using a lentiviral packaging system. A total of  $3 \times 10^5$  ACE2/HEK 293 cells were incubated with the 2.5  $\mu\text{g}/\text{ml}$  purified SARS-CoV-2-RBD labeled with biotin, and a gradient concentration of anti-SARS-CoV-2-RBD Nbs, followed by staining with streptavidin-PE (eBioscience, San Diego, CA, USA). The signals were measured by BD FACS Calibur instrument (BD Biosciences, Franklin Lakes, New Jersey, USA), and the 50% inhibitory concentration ( $\text{IC}_{50}$ ) was determined.

## 2.8 | Protein A (PA) binding assay and thermal shift assay

A total of 1 mg of Nbs was incubated with 20  $\mu\text{l}$  of Protein A chromatography resin at room temperature for 30 min. Then the mixtures were centrifuged and the protein concentration of supernatants were determined by NanoDrop. The PA binding percentage was calculated.

To determine the thermal stability of Nbs. Thermal shift assay was performed in a high-throughput manner (96-well plate) with a Q-PCR device, and 0.1 mg/ml of Nbs were mixed with 10 $\times$  Sypro Orange protein Gel stain in each tube. The program consisted of the following steps: heat to 25°C at a ramp rate of 4.4°C/s and hold for 25 s; heat to 98°C at a continuous ramp rate of 0.1°C/s; then cool to 25°C and hold for 10 s. Melting temperature ( $T_m$ ) of Nbs was measured.

## 2.9 | Authentic SARS-CoV-2 plaque reduction neutralization test (PRNT)

PRNT was used to test the blockade of SARS-CoV-2 virus attachment by Nbs. Briefly, Vero E6 cells were seeded into 24-well culture plates at  $1.5 \times 10^5$  per well and incubated at 37°C in 5%  $\text{CO}_2$  overnight. Nbs were serially diluted in DMEM supplemented with 2% FBS. The diluted SARS-CoV-2 suspension containing 300 plaque-forming units (PFU)/ml was added into Nbs, and then incubated at 37°C for 1 h. A total of 200  $\mu\text{l}$  of the Nbs-virus mixture was added into a 24-well culture plate containing Vero E6 cells. In addition, cells infected with 150 PFU/ml of SARS-CoV-2 and those without the virus were applied as positive and negative controls, respectively. After incubation for 1 h at 37°C, the Nbs-virus mixture was removed from Vero E6 cells followed by 500  $\mu\text{l}$  of DMEM with 2% FBS and 0.9% carboxymethyl cellulose (Promega) was overlaid. For further incubation at 37°C in 5%  $\text{CO}_2$  for 3 days, plaques were stained by 0.5% crystal violet. Individual plaques were counted for 50% neutralizing dose ( $\text{ND}_{50}$ ) calculation.

## 2.10 | Size-exclusion high-performance liquid chromatography, anion-exchange chromatography high-performance liquid chromatography, and reversed-phase high-performance liquid chromatography assay

Nbs were capture and purified by protein A affinity chromatography, and then further purified by hydrophobic chromatography on AKTA pure 150 (GE Healthcare, Madison, WI, USA). The purity of Nbs was detected by size exclusion chromatography–high performance liquid chromatography (SEC-HPLC), anion-exchange high-performance liquid chromatography (AEX-HPLC), and reversed-phase high-performance liquid chromatography (RP-HPLC). SEC-HPLC analysis was performed using Waters Acquity Arc system with AdvanceBio SEC 130A Columns (Agilent Technologies, Palo Alto, CA, USA), AEX-HPLC analysis was performed using Thermo Fisher Ultimate 3000 system with ProPac™ WAX-10 Columns (Thermo Scientific, Rockford, IL, USA), and RP-HPLC was performed using Thermo Fisher Ultimate 3000 system with AdvanceBio RP-mAb Diphenyl Columns (Agilent Technologies).

## 2.11 | Large-scale expression in 7-L bioreactor

The vector containing VHH gene was linearized and transformed into *Pichia pastoris* to establish a high-efficiency expression system. Dozens of clones were screened in shake flasks. After identifying the high expression clone, large-scale expression was carried out in 7-L bioreactor according to the existing fermentation method of our company. During the fermentation process, fermentation broth was sampled at different fermentation time and centrifuged by 12,000 rpm for 5 min. The supernatants of different fermentation time were tested by SDS-PAGE.

## 2.12 | Stability analysis

Formulated Nbs were stored at 4, 25, and 40°C separately. The samples stored at 4 and 25°C were examined for their purity at 2- and 4-week time points by SEC-HPLC. The samples stored at 40°C were checked at 1- and 2-week time points. The stability of samples undergone 3 and 6 freeze-and-thaw cycles were also measured.

Nbs purified from yeast fermentation at concentration of 10 mg/ml in a proper formulation were nebulized with a PARI eFlow rapid Nebulizer System (PARI GmbH, Starn-

berg, German). A total of 8 ml of formulated Nbs were filled in the reservoir and operated for about 20 min; the nebulized Nbs were collected with a 50-ml centrifugal tube. The purity of the collected Nbs was detected by SEC-HPLC.

Statistical analysis was performed using GraphPad Prism 6 software. Data are expressed as mean  $\pm$  SD.

## 3 | RESULTS

### 3.1 | Identification of Nbs specific to SARS-CoV-2 spike RBD

In order to obtain Nbs with high affinity, specificity, and good diversity, four camels were immunized with the recombinant RBD of SARS-CoV-2 spike. After seven injections at an interval of 5 days, the peripheral blood of each immunized camel was collected to construct the phage displayed library. The four libraries have more than  $10^9$  colony-forming units (CFU), and the insertion rate of each library was greater than 90%, indicating a high quality and good diversity of the four libraries. After three rounds of phage display biopanning, PE-ELISA was performed to identify binding partners of RBD. The entire schedule is illustrated in Figure 1.

In PE-ELISA assay, as shown in Figure 2A, 690 of 1600 clones were identified as positive Nbs using the criterion of a binding ratio higher than 3 compared to negative control, and most of the ELISA-positive colonies showed high binding activity to the RBD (Figure 2A). All the positive 690 Nb colonies were sequenced and the repeat sequences were removed based on the alignment of amino acid sequences. Of note, 381 RBD-specific clones with distinct sequences were identified and the phylogenetic tree analysis was performed based on the amino acid sequences of 381 Nbs by Clustal Omega (Figure 2B). Sequence analysis of the 381 distinct Nbs demonstrated substantial sequence diversity in terms of both composition and length of these sequences, which offers us more options and potential candidates in the isolation of neutralizing Nbs.

Given the RNA virus nature of SARS-CoV-2, and the reported mutations of SARS-CoV-2-RBD in different countries, cross-activity of 381 Nbs against various RBD mutants was also studied through PE-ELISA. The detailed information is provided in Figure S1. Of the 381 Nbs, 229 Nbs were identified to bind all the eight mutants (V483A, V367F, N354D, V341I, Q321L, K378R, Y508H, and H519P), and the remaining Nbs bound at least one mutant. These results demonstrated that these Nbs library could be a valuable screening resource for effective diagnostic and therapeutic reagents for COVID-19.

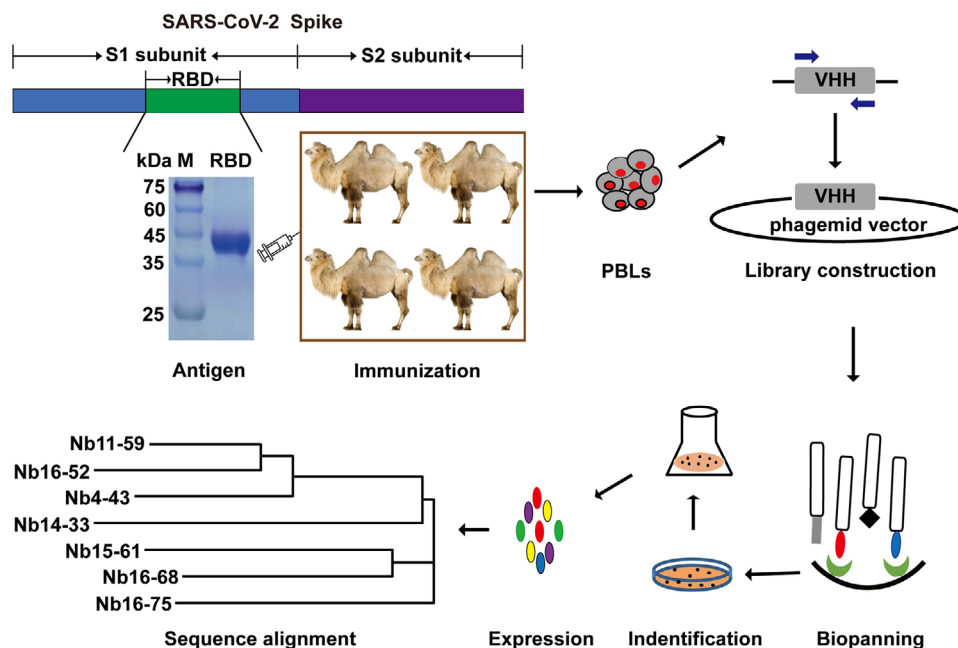


**FIGURE 1** Schematic depicting the immunization and screening strategy that were used to isolate SARS-CoV-2 Spike RBD-directed Nbs. PBLs, peripheral blood lymphocytes

### 3.2 | Identification and characterization of Nbs with SARS-CoV-2-RBD/ACE2 blocking activity

According to the cell-based blockade assay, 32 Nbs derived from lysis supernatants of 381 Nbs were considered as functional candidates, which have the ability to inhibit the interaction between RBD and ACE2, with the blocking rate higher than 15%. As indicated in Figures 3A and 3B, Nb8-87, Nb13-58, and Nb11-59 exhibited blocking rates of 16.2%, 50.4%, and 98.9%, respectively, which represented low, middle, and high inhibitory functions. In order to further study the function and characterization of the 32 Nbs, we purified these Nbs through Ni-NTA affinity chromatography. SDS-PAGE analysis of the 32 Nbs is shown in Figure 3C. The molecular weight of the 32 Nbs was all around 15 kDa, which is consistent with theoretical value. The Nbs are of high purity and could be used to study the blocking functions.

Next, we comprehensively studied the characterizations of Nbs including binding affinity, blocking activity, protein A binding activity, and  $T_m$  value. The results showed that 17 of 32 Nbs bound to SARS-CoV-2-RBD with  $EC_{50}$  lower than  $0.2 \mu\text{g/ml}$ , and 15 Nbs candidates exhibited obvious blockade effect toward SARS-CoV-2-RBD/ACE2 interaction, with  $IC_{50}$  lower than  $2 \mu\text{g/ml}$ , among which the minimal  $IC_{50}$  was  $0.580 \mu\text{g/ml}$ . Meanwhile, all Nb candidates could bind to Protein A agarose beads, with over 70% candidates showing binding efficiency higher than 80%, which

allows for a relatively easy purification process in the following large-scale manufacturing. Additionally, the  $T_m$  values of these Nb candidates ranged from  $52$  to  $58^\circ\text{C}$  (Figures 3D and Figure S2). With a comprehensive evaluation of various parameters, we eventually narrowed down to seven Nbs candidates including Nb4-43, Nb11-59, Nb14-33, Nb15-61, Nb16-52, Nb16-68, and Nb16-75. These candidates have  $EC_{50}$  and  $IC_{50}$  lower than  $0.2$  and  $1 \mu\text{g/ml}$ , respectively, as well as yield higher than  $20 \text{ mg/L}$ . Their PA binding efficacy is higher than 80% and their  $T_m$  is higher than  $57^\circ\text{C}$ . The sequences of these seven candidates were analyzed, especially the amino acid sequences of complementarity determining region 3 (CDR3), which was considered as the key and most variable region of antibody. The results were demonstrated in Figure 3E. The diversity in both composition and length among these seven Nbs provides more possibilities and alternatives to identify neutralizing Nbs.

### 3.3 | Functional study of seven Nbs against SARS-CoV-2-RBD including mutants

The seven Nbs that represented excellent binding capacity to RBD and outstanding ability to block infection were chosen to conduct comprehensive functional study on SARS-CoV-2-RBD or different RBD mutants. First, the BLI-based assay was carried out to measure the binding kinetics, and

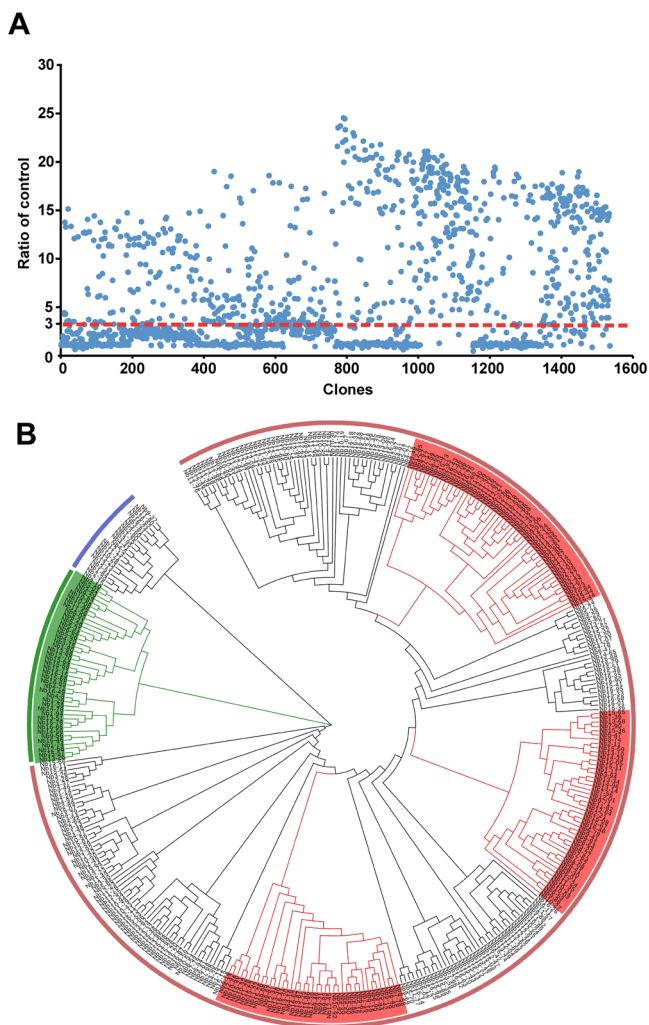


**FIGURE 2** Identification of Nbs specific to SARS-CoV-2-RBD. (A) PE-ELISA was performed to identify positive clones. The clones with binding ratio higher than 3 were considered as positive clones. (B) Phylogenetic tree of the isolated SARS-CoV-2-RBD-directed Nbs, based on the neighbor joining method

the results showed that all of these Nbs bound to SARS-CoV-2-RBD with high affinity. The  $K_d$  values ranged from 21.6 to 106 nM (Figure 4A). Almost all of the seven candidates could also bind to eight SARS-CoV-2 spike RBD mutants, including Q321L, V341I, N354D, V367F, K378R, V483A, Y508H, and H519P variants, which are circulating in the United States, England, France, and China (date not shown). Furthermore, these seven Nbs could block the interaction between ACE2 and eight different SARS-CoV-2-RBD variants (Figure 4B), with an exception of Nb16-75 that cannot bind N354D variant, suggesting N354 as an important recognizing epitope for Nb16-75 (Figure 4B).

Given that the pandemic caused by coronavirus may re-arise frequently in the next few decades, it is necessary to find anti-coronavirus drugs with broad-spectrum neutralizing activity. Hence, these seven candidates were ana-

lyzed for their neutralizing activity for other closely related beta-coronaviruses species, bat-SL-CoV-WIV1-RBD and SARS-CoV-1-RBD. Of note, two Nbs, Nb11-59 and Nb16-68, demonstrated neutralizing potency against both bat-SL-CoV-WIV1-RBD and SARS-CoV-1-RBD (Figures 4C and 4D).

### 3.4 | Nb16-68 and Nb11-59 exhibit potent neutralizing activities against authentic SARS-CoV-2

Next, the neutralizing activity of seven Nbs was determined against authentic SARS-CoV-2 in vitro. As indicated in Figure 5A, all seven Nbs exhibited a potent neutralizing ability against authentic SARS-CoV-2 in the PRNT at the concentration of 50 and 5  $\mu$ g/ml, with inhibitory rate of higher than 60% (Figures 5A and 5B). Among these seven Nbs, Nb16-68 and Nb11-59 showed the best neutralization activities. These two Nbs were serially diluted in three-fold and their antiviral potencies were determined. Nb16-68 and Nb11-59 showed a potent antiviral activity against SARS-CoV-2 in Vero E6 cells in a dose-dependent manner, as judged by decrease of phage counts, with  $ND_{50}$  of 2.2 and 0.55  $\mu$ g/ml, respectively (Figures 5C and 5D). Overall, Nb16-68 and Nb11-59 might be novel potent candidates for COVID-19 treatment.

### 3.5 | Large-scale production, stability analysis, and nebulization of humanized Nb11-59

Considering Nb11-59 exhibited the best neutralization activity toward authentic SARS-CoV-2, we selected Nb11-59 for further study. Nb11-59 was humanized according to our previous studies.<sup>14,15</sup> For future clinical application, large-scale production of SARS-CoV-2 Nb with low cost is of great necessity. Therefore, we tried to express the humanized Nb11-59 (HuNb11-59) in *P. pastoris* by fermentation. During the fermentation process in 7-L fermenter, the yield of HuNb11-59 protein increased. Surprisingly, after 213 h of induction, the yield of target protein in fermentation supernatant has even reached 20 g/L (Figure 6A), which is, to our knowledge, the highest expression of Nbs among the yield of Nbs that have been reported. After affinity chromatography and hydrophobic chromatography purification procedures, HuNb11-59 exhibited high purity through SDS-PAGE analysis (Figure 6B), and the specific purity of Nb was 99.36%, 99.55%, and 95.95%, respectively, through SEC-HPLC, AEX-HPLC, and RP-HPLC analysis (Figure 6C), which means the commercial manufacturing and purification process have been

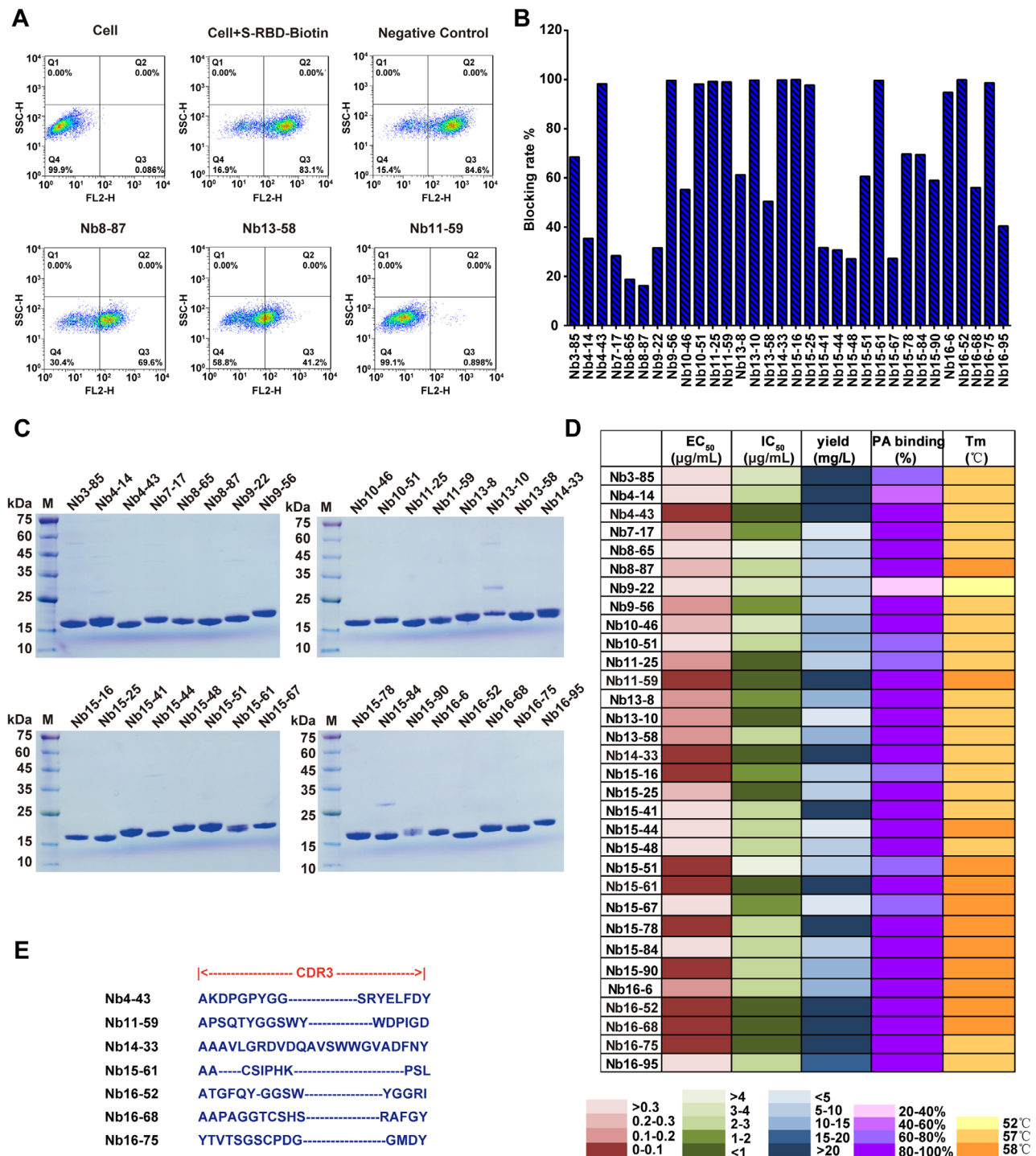


**FIGURE 3** Identification and characterization of SARS-CoV-2-RBD/ACE2 blocking Nbs. (A) Examples are given to illustrate the results of screening by FACS. (B) Screening for SARS-CoV-2-RBD/ACE2 blocking Nbs. (C) Purification of blocking SARS-CoV-2-RBD Nbs and SDS-PAGE was used to check the purity of these Nbs. (D) Characterizations of blocking Nb candidates including EC<sub>50</sub>, IC<sub>50</sub>, yield, PA binding, and T<sub>m</sub> were displayed. (E) Sequences of CDR3 region of seven selected SARS-CoV-2-RBD Nbs

successfully developed and validated, and the key methods in analytical quality characterization have been already established.

Following the successful purification of HuNb11-59 from yeast fermentation, affinity measurement and FACS-based

SARS-CoV-2-RBD/ACE2 blocking activity assay was conducted for both Nb11-59 and HuNb11-59. As shown in Figure 6D, Nb11-59 and HuNb11-59 demonstrated similar  $K_d$  value and similar profile in SARS-CoV-2-RBD/ACE2 neutralization. Furthermore, the stability of HuNb11-59

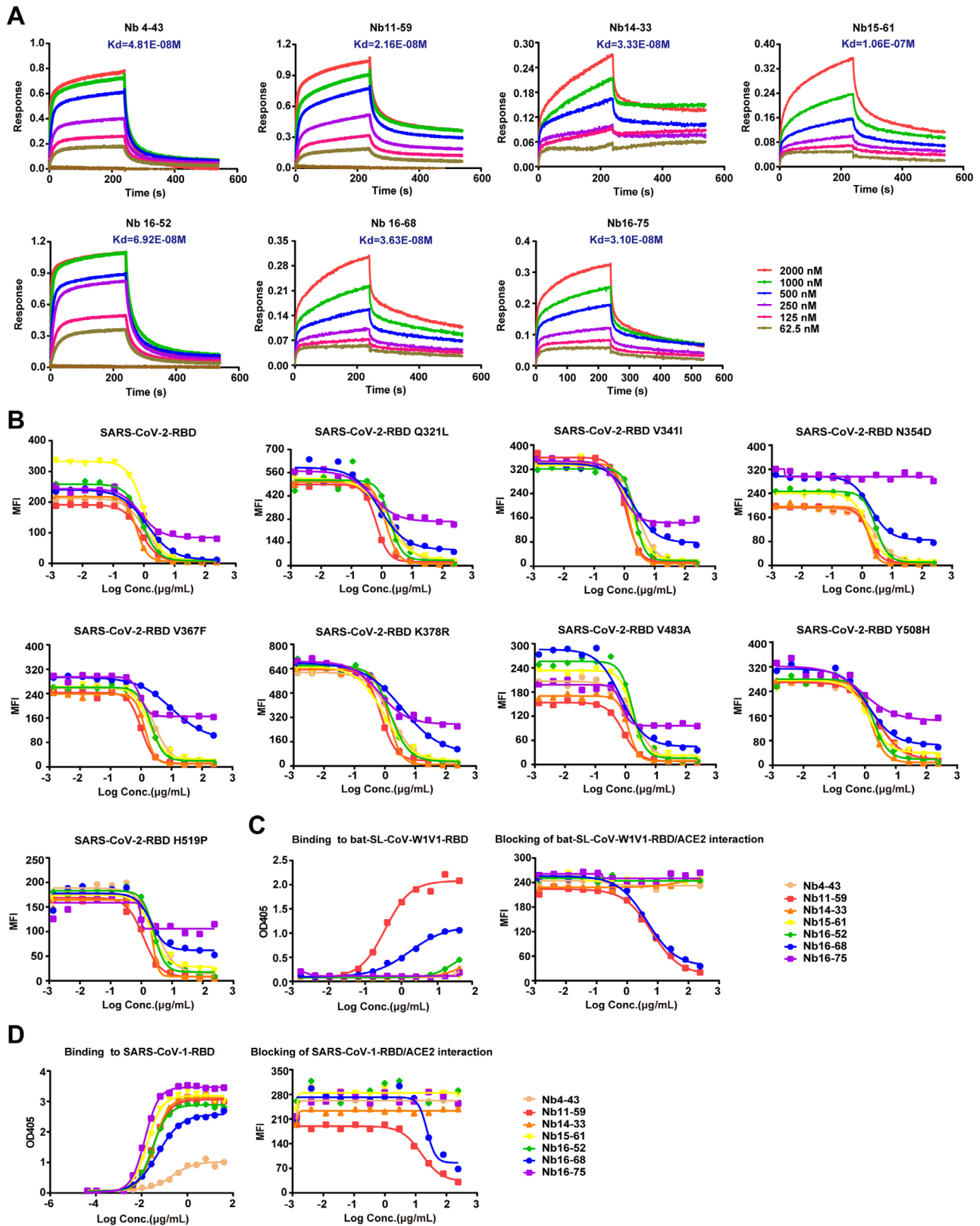


**FIGURE 4** The affinity and blocking capacity of seven Nbs toward SARS-CoV-2-RBD different mutants and other coronavirus species. (A) Affinity of selected candidates was measured by BLI. (B) The blocking activity against SARS-CoV-2-RBD mutants/ACE2 interaction was determined by FACS. (C) The binding and blocking activities of selected seven candidates toward bat-SL-CoV-W1V1-RBD were detected through ELISA and FACS, respectively. (D) The binding and blocking activities of selected seven candidates toward SARS-CoV-1-RBD were detected through ELISA and FACS, respectively

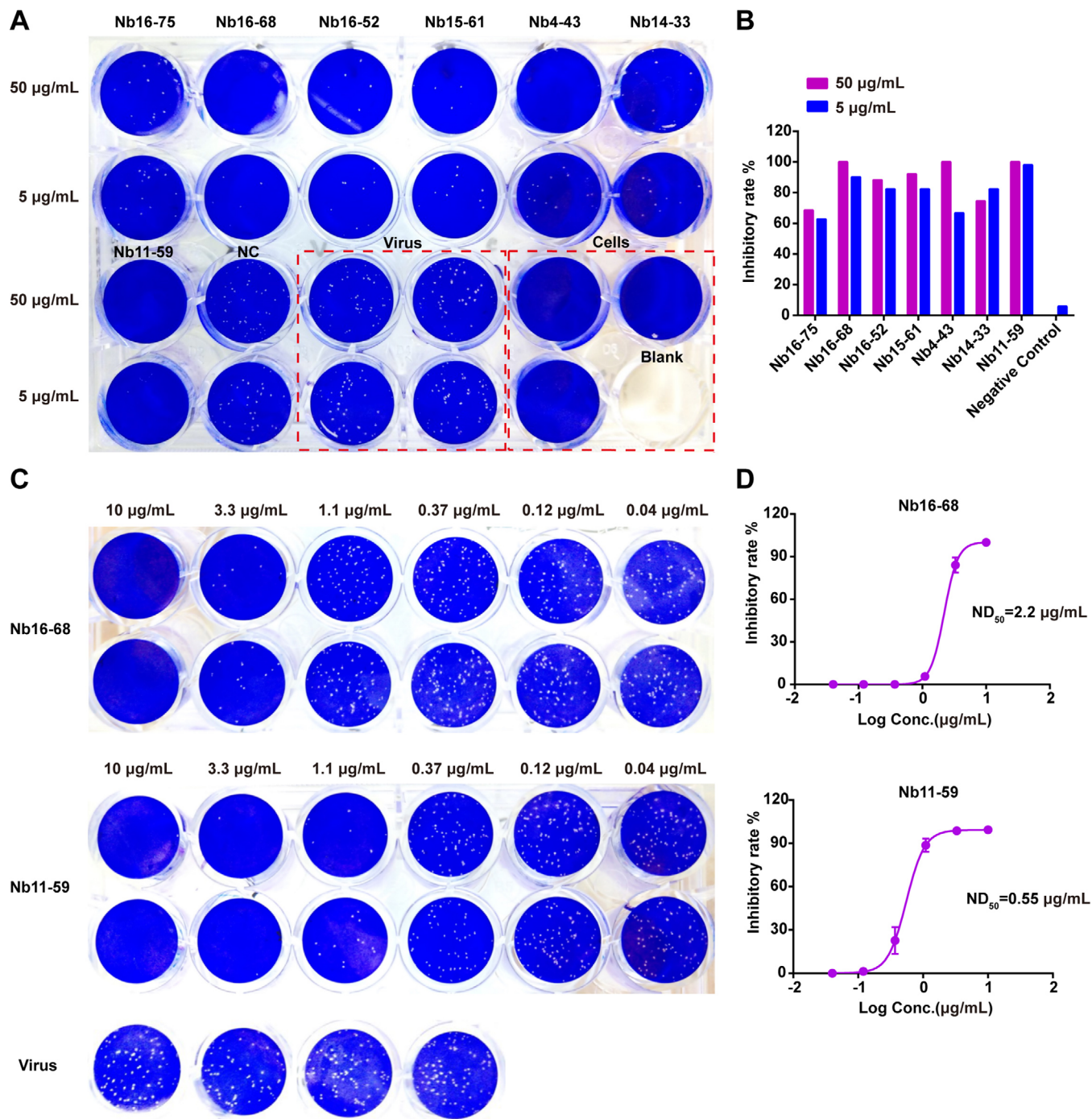


**FIGURE 5** Evaluation of neutralizing potential of seven Nbs using plaque reduction neutralization test. (A) Plaques formed in Vero E6 cells inoculated with 100 PFU SARS-CoV-2 and 10-fold diluted Nbs. Cry1B Nb was used as the negative control. (B) Inhibitory rate of seven Nbs against authentic SARS-CoV-2 at the concentration of 50 and 5  $\mu\text{g/mL}$ . (C) Plaques formed in Vero E6 cells inoculated with 100 PFU SARS-CoV-2 plus threefold diluted Nb16-68 or Nb11-59 mixture. (D) 50% ND<sub>50</sub> of Nb16-68 or Nb11-59 was determined. The results shown are mean value  $\pm$  SD

was detected at various conditions. The percentage of monomer was rather stable, maintaining above 99% when stored at 4 or 25°C for up to 4 weeks. While being left at 40°C for 2 weeks, only 0.89% degradation and 1.59% aggregation was found (Figure 6E). At the same time, a total of six cycles of freeze-and-thaw showed no effect on the

percentage of monomer (Figure 6E). These stability data showed great drug stability of HuNb11-59, which ensured the quality, safety, and efficacy of the product. In addition, The SEC-HPLC results indicated that the nebulization under formulation conditions did not significantly undermine the stability of HuNb11-59, with only a very minor

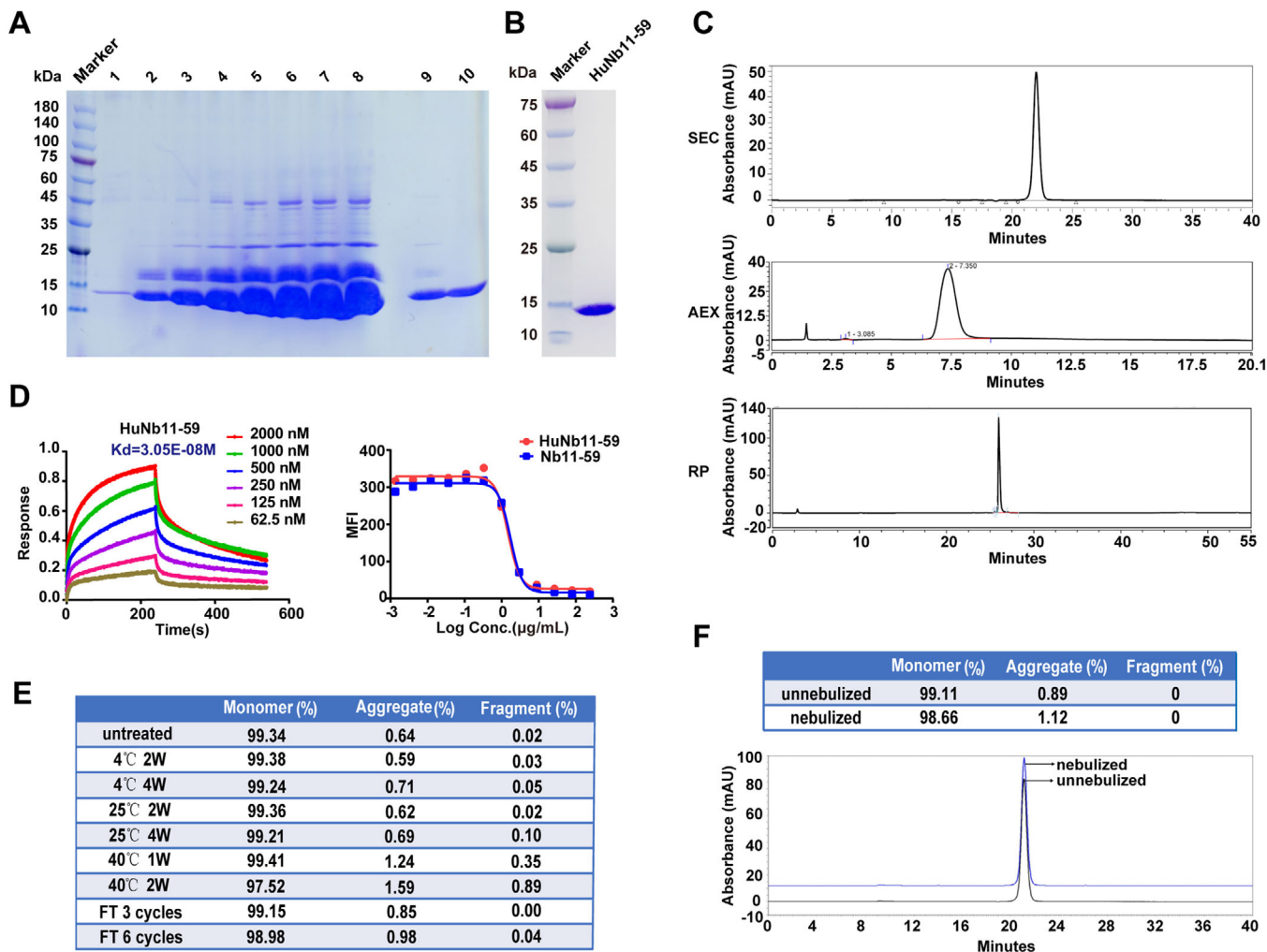


**FIGURE 6** The large-scale production and preliminary druggability analysis. (A) The yield of HuNb11-59 in fermentation tank was determined at indicated times, which were detected by SDS-PAGE assay, with 1 g/L Nb11-59 as the standard protein. Lanes 1–8, 10  $\mu$ L supernatants after 0, 24, 48, 72, 120, 159.5, 183.5, and 213 h of induction; lane 9, 10  $\mu$ L 1/20 diluted culture supernatant induced for 213 h; lane 10, 10  $\mu$ L of 1 g/L high-purity target protein. (B) The purity of HuNb11-59 was determined through SDS-PAGE, following affinity chromatography and hydrophobic chromatography. (C) The purity of HuNb11-59 was determined through SEC-HPLC, AEX-HPLC, and RP-HPLC analysis. (D) The affinity of HuNb11-59 was measured by BLI (left). The blocking activity of Nb11-59 and HuNb11-59 against SARS-CoV-2-RBD/ACE interaction was determined by FACS (right). (E) The stability of HuNb11-59 under different temperatures and freeze-and-thaw cycles was detected by SEC-HPLC. (F) The purity of nebulized HuNb11-59 formulation was detected by SEC-HPLC

proportion of aggregates found. (Figure 6F). The results demonstrated that we have creatively developed the first Nb against SARS-CoV-2 with the inhale delivery potential. The novel way of delivery may offer patients more convenient drug administration and better drug absorption effects.

## 4 | DISCUSSION

In this study, we reported Nb phage display libraries derived from four camels immunized with the SARS-

CoV-2 spike RBD, from which 381 Nbs were identified to recognize the RBD including the eight variants of SARS-CoV-2, suggesting that the RBD-specific Nbs collection could be very valuable in the development of diagnostic and therapeutic reagents for COVID-19 infection. Currently, Nb-based diagnostic methods have not been reported yet. It would be very meaningful to develop SARS-CoV-2 virus fast-tracking techniques with Nbs.<sup>16</sup> In addition to the diagnostic value, Nbs could also be developed as PET-CT probes for their good tissue infiltration ability and short half-life in vivo.<sup>17</sup> The large RBD-specific Nb library in this study would facilitate

the screening for COVID-19 preventive and therapeutic candidates.

The published neutralizing Nbs toward SARS-CoV-2 were evaluated mainly in the pseudovirus system, with  $IC_{50}$  ranging from 0.003 to 12.32  $\mu\text{g}/\text{ml}$ .<sup>10,18–21</sup> Of note,  $IC_{50}$  of molecules tested in the pseudovirus system might be two- to 100-fold lower than that in the authentic SARS-CoV-2.<sup>19,22</sup> We identified a potently neutralizing molecule of Nb11-59, which recognizes the wild-type and eight kinds of mutants of RBD proteins. Nb11-59 was capable of inhibiting the replication of authentic SARS-CoV-2 in vitro with  $ND_{50}$  of 0.55  $\mu\text{g}/\text{ml}$ , which is similar to or lower than the  $ND_{50}$  or  $IC_{50}$  values of several reported mAbs isolated from human B cells.<sup>3,22,23</sup> Notably, Nb11-59 demonstrates higher neutralizing abilities than some reported Nbs, including n3130 and n3088 with  $IC_{50}$  of 4.0 and 2.6  $\mu\text{g}/\text{ml}$ , respectively, against authentic SARS-CoV-2.<sup>24</sup> In our next study, Nb11-59 needs to be further studied in the safety and efficacy in animals.

With the continuing COVID-19 epidemic, the resistance to any potential antiviral therapeutic would be the focus due to the rapid mutation of viral pathogens, especially under the selective pressure of antiviral drugs. Indeed, naturally occurring RBD variations, such as V483A, V367F, and V341I variants, have been circulating in some regions of the world.<sup>25</sup> A number of drugs, especially RBD-directed antibodies with potent neutralizing activities against SARS-CoV-2, have been described.<sup>25</sup> Nevertheless, there are few reports about antibodies that can neutralize a wide range of SARS-CoV-2 variants. Herein, we showed that seven RBD-directed Nbs identified were capable of blocking the interaction between ACE2 and the eight RBD-mutant variants, with Nb11-59 showing the most potent blocking activities. In addition, these molecules also demonstrate blocking activities against SARS-CoV-1 and bat-SL-CoV-WIV1. Further study needs to be performed for evaluating the neutralizing activities against authentic SARS-CoV-2 variants. Notably, the variants resistant to these molecules would likely arise under the selective pressure, although they might have broad spectrum activities against the different SARS-CoV-2 variants. Noncompeting antibody cocktail treatment might be a good strategy to prevent rapid mutational escape of SARS-CoV-2.<sup>26</sup>

The development of vaccines and mAbs represents a promising strategy for combating COVID-19 infections, however, they might induce antibody-dependent enhancement (ADE), an undesirable phenomenon that leads to increased infectivity and virulence, which has been observed in the infection of SARS-CoV-1, MERS-COV, HIV, and Ebola viruses with the treatment of nonneutralizing or neutralizing mAbs.<sup>27–30</sup> It is known that ADE is likely to be associated with Fc domain of antibodies. Despite the sub-

stantial attempts made at the modifications of Fc domains to avoid the emergence of ADE, the expected results have not been achieved.<sup>31,32</sup> Because of lacking Fc domain, Nbs or VHHs represent ideal neutralizing antibodies against viral infections. A typical example is Nb ALX-0171 with potent neutralizing activities against respiratory syncytial virus, which is currently in phase II clinical trials.<sup>33</sup> Therefore, the development of neutralizing Nbs that do not contain Fc domains has significant advantages in the fight against COVID-19.

Considering their small size and biophysical properties, single-domain antibodies have multiple advantages in the treatment of respiratory tract infectious diseases. First, single-domain antibodies could be produced on a large scale at low cost. We showed that Nb11-59 expression could reach 20 g/L through fermentation using the yeast expression system, which means that it could be rapidly and widely used as a preventive or therapeutic molecule. Second, Nb11-59, as a single domain antibody with small size, could be delivered to the site of infection via inhalation, which is supported by its high stability at the temperature ranging from 4 to 40°C, and its consistent post-nebulization stability profile. Because of the highly infectious and continuous outbreak of COVID-19, the inhaled delivery of Nb11-59 is likely effective in controlling the spread of the virus. Taken together, Nb11-59 is a very potential therapeutic molecule against COVID-19, and it is worthy of further research to facilitate rapid clinical development.

## ACKNOWLEDGMENTS

We thank Jia Wu, Jun Liu, and Hao Tang from BSL-3 Facility of Wuhan Institute of Virology for their essential support. We thank Center for Biosafety Mega-Science, Chinese Academy of Sciences and the National Virus Resource Center for resource support. We also thank Hongde Liu from Southeast University offers the assistance. This work was funded by National Natural Science Foundation of China (81902052), Shanghai Sailing Program (20YF1434300), and the Natural Science Foundation of Hubei Province of China (2019CFA076).

## CONFLICT OF INTEREST

All commercial rights from this paper belong to Shanghai Novamab Biopharmaceuticals Co., Ltd.

## AUTHOR CONTRIBUTIONS

Yakun Wan conceptualized and designed the study. Junwei Gai, Linlin Ma, Guanghui Li, Min Zhu, Peng Qiao, Xiaofei Li, and Haiwei Zhang developed the methodology. Junwei Gai, Guanghui Li, Peng Qiao, Xiaofei Li, Haiwei Zhang, Yanmin Zhang, Yadong Chen, Weiwei Ji, Hao Zhang, Huanhuan Cao, and Xionghui Li collected

the data. Junwei Gai, Linlin Ma, Guanghui Li, and Min Zhu analyzed and interpreted the data. Linlin Ma, Yakun Wan, Junwei Gai, and Guanghui Li wrote, reviewed, and revised the manuscript. Yakun Wan, Rui Gong, and Min Zhu supervised the study.

### ETHICS APPROVAL

The animal experiments were approved by the Animal Experimental Ethics Committee of Shanghai University of Medicine and Health Sciences.

### DATA AVAILABILITY STATEMENT

The data that support the findings of this study are available from the corresponding author upon reasonable request.

### REFERENCES

- Zhang T, Wu Q, Zhang Z. Probable pangolin origin of SARS-CoV-2 associated with the COVID-19 outbreak. *Curr Biol*. 2020;30(7):1346-1351.
- Zhang Y-Z, Holmes EC. A genomic perspective on the origin and emergence of SARS-CoV-2. *Cell*. 2020;181(2):223-227.
- Chi X, Yan R, Zhang J, et al. A neutralizing human antibody binds to the N-terminal domain of the Spike protein of SARS-CoV-2. *Science*. 2020;369(6504):650-655.
- Yuan M, Wu NC, Zhu X, et al. A highly conserved cryptic epitope in the receptor binding domains of SARS-CoV-2 and SARS-CoV. *Science*. 2020;368(6491):630-633.
- Yan R, Zhang Y, Li Y, Xia L, Guo Y, Zhou Q. Structural basis for the recognition of SARS-CoV-2 by full-length human ACE2. *Science*. 2020;367(6485):1444-1448.
- Lan J, Ge J, Yu J, et al. Structure of the SARS-CoV-2 spike receptor-binding domain bound to the ACE2 receptor. *Nature*. 2020;581(7807):215-220.
- Van Audenhove I, Gettemans J. Nanobodies as versatile tools to understand, diagnose, visualize and treat cancer. *EBioMedicine*. 2016;8:40-48.
- Wang Y, Fan Z, Shao L, et al. Nanobody-derived nanobiotechnology tool kits for diverse biomedical and biotechnology applications. *Int J Nanomedicine*. 2016;11:3287-3303.
- Van Heeke G, Allosery K, De Brabandere V, De Smedt T, Detalle L, de Fougerolles A. Nanobodies® as inhaled biotherapeutics for lung diseases. *Pharmacol Ther*. 2017;169:47-56.
- Wrapp D, De Vlioger D, Corbett KS, et al. Structural basis for potent neutralization of betacoronaviruses by single-domain camelid antibodies. *Cell*. 2020;181(5):1004-1015.
- Zhou P, Yang X-L, Wang X-G, et al. A pneumonia outbreak associated with a new coronavirus of probable bat origin. *Nature*. 2020;579(7798):270-273.
- Li G, Zhu M, Ma L, et al. Generation of small single domain nanobody binders for sensitive detection of testosterone by electrochemical impedance spectroscopy. *ACS Appl Mater Interfaces*. 2016;8(22):13830-13839.
- Madeira F, Park YM, Lee J, et al. The EMBL-EBI search and sequence analysis tools APIs in 2019. *Nucleic Acids Res*. 2019;47(W1):W636-W641.
- Ma L, Zhu M, Gai J, et al. Preclinical development of a novel CD47 nanobody with less toxicity and enhanced anti-cancer therapeutic potential. *J Nanobiotechnol*. 2020;18(1):12.
- Xian Z, Ma L, Zhu M, et al. Blocking the PD-1-PD-L1 axis by a novel PD-1 specific nanobody expressed in yeast as a potential therapeutic for immunotherapy. *Biochem Biophys Res Commun*. 2019;519(2):267-273.
- Mir MA, Mehraj U, Sheikh BA, Hamdani SS. Nanobodies: the “magic bullets” in therapeutics, drug delivery and diagnostics. *Hum Antibodies*. 2020;28(1):29-51.
- Keyaerts M, Xavier C, Heemskerk J, et al. Phase I study of 68Ga-HER2-nanobody for PET/CT assessment of HER2 expression in breast carcinoma. *J Nucl Med*. 2016;57(1):27-33.
- Li D, Li T, Cai H, et al. Potent synthetic nanobodies against SARS-CoV-2 and molecular basis for neutralization. *bioRxiv*. 2020. <https://doi.org/10.1101/2020.06.09.143438>.
- Chi X, Liu X, Wang C, et al. Humanized single domain antibodies neutralize SARS-CoV-2 by targeting spike receptor binding domain. *bioRxiv*. 2020. <https://doi.org/10.1101/2020.04.14.042010>.
- Custodio TF, Das H, Sheward DJ, et al. Selection, biophysical and structural analysis of synthetic nanobodies that effectively neutralize SARS-CoV-2. *bioRxiv*. 2020. <https://doi.org/10.1101/2020.06.23.165415>.
- Hanke L, Vidakovics MLP, Sheward D, et al. An alpaca nanobody neutralizes SARS-CoV-2 by blocking receptor interaction. *bioRxiv*. 2020. <https://doi.org/10.1101/2020.06.02.130161>.
- Cao Y, Su B, Guo X, et al. Potent neutralizing antibodies against SARS-CoV-2 identified by high-throughput single-cell sequencing of convalescent patients' B cells. *Cell*. 2020;182(1):73-84.
- Wu Y, Wang F, Shen C, et al. A noncompeting pair of human neutralizing antibodies block COVID-19 virus binding to its receptor ACE2. *Science*. 2020;368(6496):1274-1278.
- Wu Y, Li C, Xia S, et al. Identification of human single-domain antibodies against SARS-CoV-2. *Cell Host Microbe*. 2020;27(6):891-898.
- Ou J, Zhou Z, Dai R, et al. Emergence of RBD mutations in circulating SARS-CoV-2 strains enhancing the structural stability and human ACE2 receptor affinity of the spike protein. *bioRxiv*. 2020. <https://doi.org/10.1101/2020.03.15.991844>.
- Baum A, Fulton BO, Wloga E, et al. Antibody cocktail to SARS-CoV-2 spike protein prevents rapid mutational escape seen with individual antibodies. *Science*. 2020;369(6506):1014-1018.
- Wang S-F, Tseng S-P, Yen C-H, et al. Antibody-dependent SARS coronavirus infection is mediated by antibodies against spike proteins. *Biochem Biophys Res Commun*. 2014;451(2):208-214.
- Wan Y, Shang J, Sun S, et al. Molecular mechanism for antibody-dependent enhancement of coronavirus entry. *J Virol*. 2020;94(5):e02015-02019.
- Wiley S, Aasa-Chapman MM, O'Farrell S, et al. Extensive complement-dependent enhancement of HIV-1 by autologous non-neutralising antibodies at early stages of infection. *Retrovirology*. 2011;8(1):16.
- Takada A, Feldmann H, Ksiazek TG, Kawaoka Y. Antibody-dependent enhancement of Ebola virus infection. *J Virol*. 2003;77(13):7539-7544.

31. Thommesen JE, Michaelsen TE, Løset GÅ, Sandlie I, Brekke OH. Lysine 322 in the human IgG3 CH2 domain is crucial for antibody dependent complement activation. *Mol Immunol.* 2000;37(16):995-1004.
32. Hessel AJ, Hangartner L, Hunter M, et al. Fc receptor but not complement binding is important in antibody protection against HIV. *Nature.* 2007;449(7158):101-104.
33. Xing Y, Proesmans M. New therapies for acute RSV infections: where are we? *Eur J Pediatr.* 2019;178(2):131-138.

## SUPPORTING INFORMATION

Additional supporting information may be found online in the Supporting Information section at the end of the article.

**How to cite this article:** Gai J, Ma L, Li G, et al. A potent neutralizing nanobody against SARS-CoV-2 with inhaled delivery potential. *MedComm.* 2021;2:101–113. <https://doi.org/10.1002/mco2.60>